Compensation for the Effects of Mutual Coupling on Direct Data Domain Adaptive Algorithms

Raviraj S. Adve, *Member, IEEE,* and Tapan Kumar Sarkar, *Fellow, IEEE*

***Abstract*—This paper investigates the effects of mutual coupling between the elements of an array on direct data domain algorithms. Mutual coupling severely undermines the interference suppression capabilities of direct data domain algorithms. The method of moments (MoM) is used to evaluate the mutual coupling between the elements of a given array. The MoM admittance matrix is then used to eliminate the effects of mutual coupling.**

***Index Terms*—Adaptive arrays, mutual coupling.**

I. Introduction

ADAPTIVE array techniques promise to be the best means available to mitigate the effects of severe dynamic interference on the performance of airborne radar systems. The principle advantage of an adaptive array is the ability to electronically steer the mainlobe of the antenna to any desired direction while also automatically placing deep pattern nulls in the specific direction of interference sources.

Most proposed adaptive algorithms are based on the covariance matrix of the interference [1]. However, these statistical algorithms suffer from two major drawbacks. First, they require independent identically distributed secondary data to estimate the covariance matrix of the interference. Unfortunately, in airborne early warning radar applications, the statistics of the interference may fluctuate rapidly over a short distance limiting the availability of homogeneous secondary data. The resulting errors in the covariance matrix reduces the ability to suppress interference. The second drawback is that the estimation of the covariance matrix requires the storage and processing of the secondary data. This is computationally intensive, requiring many calculations in real time.

Recently, direct data domain algorithms have been proposed to overcome these drawbacks of statistical techniques [2]–[4]. The approach is to adaptively minimize the interference power while maintaining array gain in the direction of the signal. Not having to estimate a covariance matrix eliminates the sample support problem and leads to enormous savings in required real time computations.

As proposed, most adaptive algorithms assume that the elements of receiving array are independent isotropic point sensors that sample, but do not reradiate, the incident fields. It is further assumed that the array is isolated from its surroundings. However, in a real system, each array element must have some physical size. In the practical case, the elements spatially sample and reradiate the incident fields. The reradiated fields interact with the other elements causing the sensors to be mutually coupled. It must be mentioned that while this paper focuses only on the effects of mutual coupling on the performance of adaptive algorithms, a similar effect is seen due to scattering from objects in the near field of the array. For example, in an airborne radar application, the scatterer could be wing of the aircraft platform.

Gupta and Ksienski [5] analyze and compensate for the effects of mutual coupling on a statistical adaptive algorithm. The analysis is restricted to a linear array of thin half-wavelength dipoles. The authors define the mutual coupling as the mutual impedance of two such dipoles and demonstrate that even for large interelement spacing, mutual coupling degrades the ability of statistical algorithms to suppress interference [6]. Adve [7] reports a similar degradation in the capabilities of direct data domain algorithms.

In [5] the authors compensate for the effects of mutual coupling by relating the open circuit voltages (voltages at the ports of the array if all were open circuited) with the voltages measured at the ports. The stated assumption is that open-circuit voltages are free of mutual coupling. This assumption is only valid in a limited sense. The open circuit voltages are the voltages in the presence of the other open circuited elements. As shall be shown in this paper, this implies that the effects of mutual coupling have been reduced but not eliminated.

The work of [5] remains the only published effort analyzing the effects of and compensating for mutual coupling in adaptive antenna arrays used for signal recovery. Many authors have used this formulation to analyze and eliminate the effects of mutual coupling on direction of arrival (DOA) estimation algorithms [8], [9]. Pasala and Friel [11] use the method of moments (MoM) to quantize and eliminate the effects of mutual coupling on DOA estimation algorithms. However, the authors solve the entire MoM problem, requiring knowledge of the incident fields. In practice, this information is not available.

In the present work, the problem of signal recovery by a linear array of equispaced thin half-wavelength dipoles is analyzed. The MoM is used to analyze the antenna array. For an accurate analysis, multiple basis functions (unknowns) per element are used. Using a Galerkin formulation, the entries of the MoM impedance matrix measure the interaction between the basis functions, i.e., they quantize the mutual coupling. In contrast, the work of [5] is equivalent to using one basis function per element in a MoM analysis. This is well known to be inadequate for an accurate numerical analysis.

Manuscript received May 8, 1996; revised December 14, 1998. This work was supported in part by AFRL Sensors Directorate under Grant F30602-95-1-0014 and by NSF under Grant ECS-9901361.

R. S. Adve is with the Research Associates for Defense Conversion, Marcy, NY 13403 USA.

T. K. Sarkar is with the Division of Electrical Engineering and Computer Science, Syracuse University, Syracuse, NY 13244 USA.

Publisher Item Identifier S 0018-926X(00)01268-0.

In Section II, the antenna is modeled as a linear array of identical, thin, centrally point loaded dipoles. The MoM is then used to analyze the behavior of the array in the presence of an arbitrary incident field. This analysis leads to the MoM impedance matrix. While MoM analyses of wire dipoles are well known, the formulation is presented here to obtain the exact relationship between the incident fields with the measured voltages. This formulation will be crucial to the elimination of mutual coupling.

In Section III, the effects of mutual coupling on the performance of a direct data domain algorithm of Sarkar and Sangruji [2] are illustrated using two examples. Section IV presents a technique to compensate for the effects of mutual coupling. The proposed technique is tested on the examples of Section III. The technique is also compared to the compensation for mutual coupling using open circuit voltages as suggested by [5]. Another example is also presented to present the ability of the technique to suppress interference in different scenarios.

II. Method of Moments Analysis

In an adaptive receiving system, an antenna array receives a signal corrupted by thermal noise and possibly external interference such as clutter and jammers. From an electromagnetics point of view, this can be treated as multiple incident fields impinging on the antenna. To understand the behavior of the antenna, we must therefore analyze its response to an arbitrary incident field.

In this paper, the receiving antenna is assumed to be a linear array of N_e elements. The elements are parallel thin equispaced dipoles. Each element of the array is identically point loaded at the center. The dipoles are z-directed, of length L and radius a, and are placed along the x-axis, separated by distance Δx. The array lies in the X-Z plane.

We begin by analyzing the response of the antenna array to a incident field $\mathbf{E^{inc}}$. Since the array is composed of thin wires the following simplifying assumptions are valid [14]: 1) the current flows only in the direction of the wire axes (here the z direction.); 2) The current and charge densities on the wire are approximated by filaments of current and charge on the wire axes (that lie in the $y = 0$ plane); and 4) surface boundary conditions can be applied to the relevant axial component on the wire axes.

Based on these assumptions, the integral equation that relates the incident field to the current on the wires and describes the behavior of the array is

$$E_z^{\rm inc} = -\mu_0 \int_{\rm axes} I(z') \frac{e^{-jkR}}{4\pi R} dz' + \frac{1}{\epsilon_0} \frac{\partial}{\partial z} \int_{\rm axes} \frac{\partial I(z')}{\partial z'} \frac{e^{-jkR}}{4\pi R}\, dz'. \tag{1}$$

We solve this equation using the MoM to obtain the MoM impedance matrix. The basis functions used are piecewise sinusoids as described in [13] and shown in Figs. 1 and 2. P (chosen odd) basis functions are used per element. Using these basis functions and a Galerkin formulation, (1) is reduced to the matrix equation

$$[V] = [\mathbf{Z}][I] \Rightarrow [I] = [\mathbf{Y}][V] \tag{2}$$

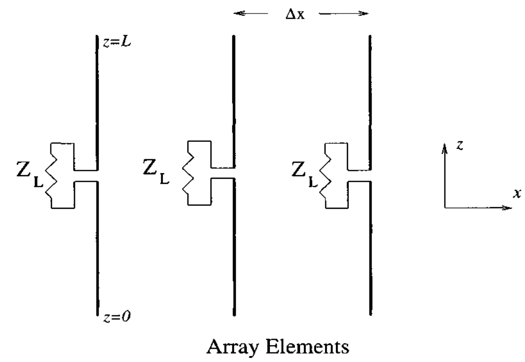

Fig. 1. Model of the receiving antenna as a linear array.

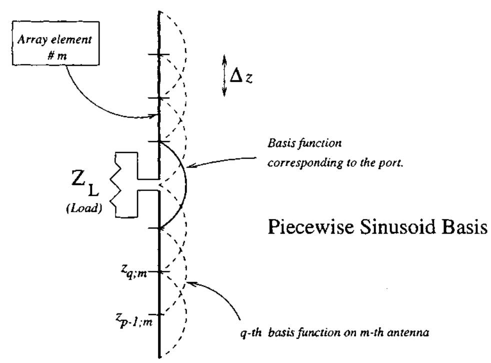

Fig. 2. Basis functions used in the MoM.

where $[I]$ is the MoM current vector with the coefficients of the expansion of the current in the sinusoidal basis. $[V]$ is the MoM voltage vector representing the inner product of the weighting functions and the incident field. [**Z**] and [**Y**] are the MoM impedance and admittance matrices respectively. Both matrices are of order $N \times N$, where $N = N_e P$ is the total number of unknowns used in the MoM formulation.

Assuming that the incident field is linearly polarized and arrives from direction (θ, ϕ), it can be written in the functional form

$$E_z^{\rm inc} = E_0 e^{-j\mathbf{k}.\mathbf{r}} \tag{3}$$

where $\mathbf{k} = -k[\hat{\mathbf{a}}_x \cos\phi \sin\theta + \hat{\mathbf{a}}_y \sin\phi \sin\theta + \hat{\mathbf{a}}_z \cos\theta]$ is the wave vector associated with the direction of arrival of the incident signal. Therefore, the ith entry in the MoM voltage vector $[V]$, corresponding to the qth basis function on the mth antenna, is given by the analytic form

$$V_i = \frac{E_0 e^{jk(m-1)\Delta x \cos\phi \sin\theta}}{2} e^{jkz_{q,m}\cos\theta} k \sin(k\Delta z) \sin^2\theta \cdot [\cos(k\Delta z \cos\theta) - \cos(k\Delta z)] \tag{4}$$

where $i = (m-1)P + q$, $\Delta z = z_{q;m} - z_{q-1;m}$. $z_{q;m}$ is defined in Fig. 2.

The i, lth entry in the [**Z**] matrix is the inner product of the ith basis function $(f_{q,m})$ with the z-component of the electric field due to a sinusoidal current source corresponding to the lth basis function $(f_{p,n}, l = (p-1)P + n)$. Therefore, the entries of the [**Z**] matrix are a measure of the interaction between different sections of the antenna array; that is, they are a measure of the mutual coupling between sections of the array. An analytic expression for the entries of the MoM impedance matrix is derived in [13].

Because of the choice of a piecewise sinusoid basis and the choice of an odd number of basis functions per antenna element, only one basis function is nonzero at the port. This is illustrated in Fig. 2 where the basis function marked in bold is the only one contributing to the current at the port. Therefore, the measured voltage at the port of the nth antenna is given by

$$V_{\text{meas}_\text{m}} = Z_L I_{(P+1/2),m} \tag{5}$$

i.e., the measured voltage at a port of the array is directly proportional to the coefficient of the basis function corresponding to the that port.

The next section illustrates the effects of mutual coupling by comparing the ideal case of no mutual coupling between antenna elements with the case where mutual coupling is taken into account, but not compensated for. The effects are demonstrated on a direct-data domain algorithm.

III. The Effects of Mutual Coupling

In [2], Sarkar and Sangruji present a direct data domain technique to adaptively recover a desired signal arriving from a given look direction while simultaneously rejecting all other interference. The technique is based on the fact that in the absence of mutual coupling, a far-field source presents a linear phase front at the ports of a linear array. In this section, we demonstrate that the mutual coupling undermines the ability of this algorithm to maintain the gain of the array in the direction of the signal while simultaneously rejecting the interference. To do so, we compare the performance of the algorithm in the ideal case of mutual coupling with the case where mutual coupling is taken into account but not compensated for. We begin by briefly describing the adaptive technique developed in [2].

A. Least Squared Error Adaptive Nulling

Consider an array of N_e uniformly spaced isotropic point sensors shown in Fig. 3. The array receives a signal (marked S) from an assumed direction ϕ_0 and some interference sources (marked J_i) from unknown directions. In the absence of mutual coupling, each individual source presents a linear phase progression across the face of the array. Therefore, the voltage at the ith element due to the incident fields is

$$V_i = Se^{jk(i-1)\Delta x u_0} + \sum_{m=1}^{M_s} J_m e^{jk(i-1)\Delta x u_m} + n_i, \quad i = 1, \cdots, N_e \tag{6}$$

where $u_m = \cos\phi_m$, S is the complex intensity of the signal incident from direction ϕ_0, J_m is the intensity of the mth interference source arriving from direction ϕ_m, and n_i is the additive noise at each element. Let $\beta = \exp(jk\Delta x u_0)$ represent the phase progression of the signal between one element and the next. Hence, the term $V_i - \beta^{-1}V_{i+1}$ has no signal component. Consider the $K \times K$ matrix equation given by

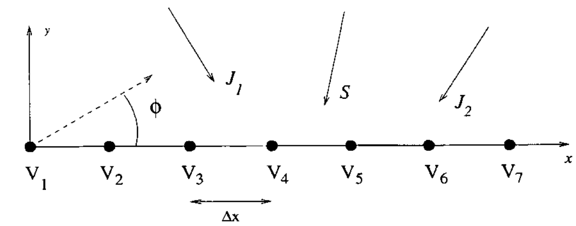

Fig. 3. Model of array comprised of isotropic point sensors.

$$\begin{bmatrix} 1 & \beta & \cdots & \beta^{K-1} \\ V_1 - \beta^{-1}V_2 & V_2 - \beta^{-1}V_3 & \cdots & V_K - \beta^{-1}V_{K+1} \\ V_2 - \beta^{-1}V_3 & V_3 - \beta^{-1}V_4 & \cdots & V_{K+1} - \beta^{-1}V_{K+2} \\ \vdots & \vdots & \vdots & \vdots \\ V_{K-1} - \beta^{-1}V_K & V_K - \beta^{-1}V_{K+1} & \cdots & V_{N_e-1} - \beta^{-1}V_{N_e} \end{bmatrix} \cdot \begin{bmatrix} w_1 \\ w_2 \\ w_3 \\ \vdots \\ w_K \end{bmatrix} = \begin{bmatrix} 1 \\ 0 \\ 0 \\ \vdots \\ 0 \end{bmatrix} \tag{7}$$

where $K = (N_e + 1)/2$. The last $K - 1$ rows of the matrix contain only interference and noise terms. Setting the product of these terms with the weights to zero, nulls the interference in a least squared sense. The equation represented by the first row constrains the array gain in the direction of the signal. It can be shown that if $M + 1 \leq K$, the signal can be recovered and

$$S = \sum_{i=1}^{K} w_i V_i. \tag{8}$$

B. Numerical Examples

Two examples demonstrate the effect of mutual coupling between the elements of the array on the algorithm described in Section III-A. In each example, an array receives a signal corrupted by three jammers. To focus only on the effects of mutual coupling these examples neglect thermal noise.

For each example two scenarios are compared. In the first scenario the ideal case of no mutual coupling is assumed and the voltages at the array ports are given by (6). These voltages are then passed to the signal recovery subroutine to find the weights using (7) and the signal is estimated using (8).

In the second scenario the mutual coupling is taken into account. The antenna is analyzed using the MoM. The intensities of the signal and interference and their directions of arrival in conjunction with (4) are used to calculate the MoM voltage vector. Equation (5) is used to find the voltages that are measured across the load at the individual ports. These measured voltages are input to the signal recovery subroutine. The signal intensity is then recovered using (8). No attempt is made to compensate for mutual coupling.

The details of the chosen array are presented in Table I. The receiving algorithm tries to maintain the gain of the array in the

TABLE I
DETAILS OF EXAMPLE ARRAY

Number of elements in array	7
Length of z−directed wires	$\frac{\lambda}{2}$
Radius of wires	$\frac{\lambda}{200}$
Spacing between wires	$\frac{\lambda}{2}$
Loading at the center	50Ω

TABLE II
BASE SIGNAL AND JAMMER VALUES

	Magnitude	Phase	DOA
Signal	1.0 V/m	0.0	45^o
Jammer # 1	1.0 V/m	0.0	75^o
Jammer # 2	1.5 V/m	0.0	60^o
Jammer # 3	2.0 V/m	0.0	30^o

direction of $\phi_0 = 45°$ while automatically placing nulls at in the interference directions. All signals and jammers arrive from the elevation $\theta = 90°$. The base signal and jammer intensities and directions of arrival are given in Table II.

In all simulations the jammer intensities, the directions of arrival of the jammers and the signal intensity are used only to find the voltages input to the receiving algorithm. The receiving algorithm itself uses only the direction of arrival of the signal, i.e., only the look direction is considered to be known.

C. Example 1: Constant Jammers

In the first example, the magnitude of the incident signal is varied from 0 V/m to 10.0 V/m in steps of 0.05 V/m while maintaining the jammer intensities constant as given in Table II. If the jammers have been nulled correctly and the signal recovered properly, it is expected that the recovered signal has a linear relationship with respect to the intensity of the incident signal.

Fig. 4(a) plots the results of using the algorithm presented in Section III-A to recover the signal in the presence of jammers in the absence of mutual coupling. As can be seen, this magnitude displays the expected linear relationship.

In the second scenario, for each value of the incident signal intensity, mutual coupling is taken into account and the measured voltages are obtained using the MoM. The results of the reconstruction using the voltages affected by mutual coupling are presented in Fig. 4(b). As can be seen from the figure, in the presence of mutual coupling the reconstruction is completely inaccurate. As the incident signal increases in intensity, the reconstructed signal displays a nonlinear behavior.

In the above example, jammers are included in the simulation to illustrate the effects of mutual coupling on interference suppression. Without any interference, the plot of reconstructed signal versus intensity of incident signal is would be the linear relationship of Fig. 4(a). This is because in the absence of mutual coupling the beam pattern would change little with changing signal strength. Most of the signal is eliminated by the subtraction operation in (7).

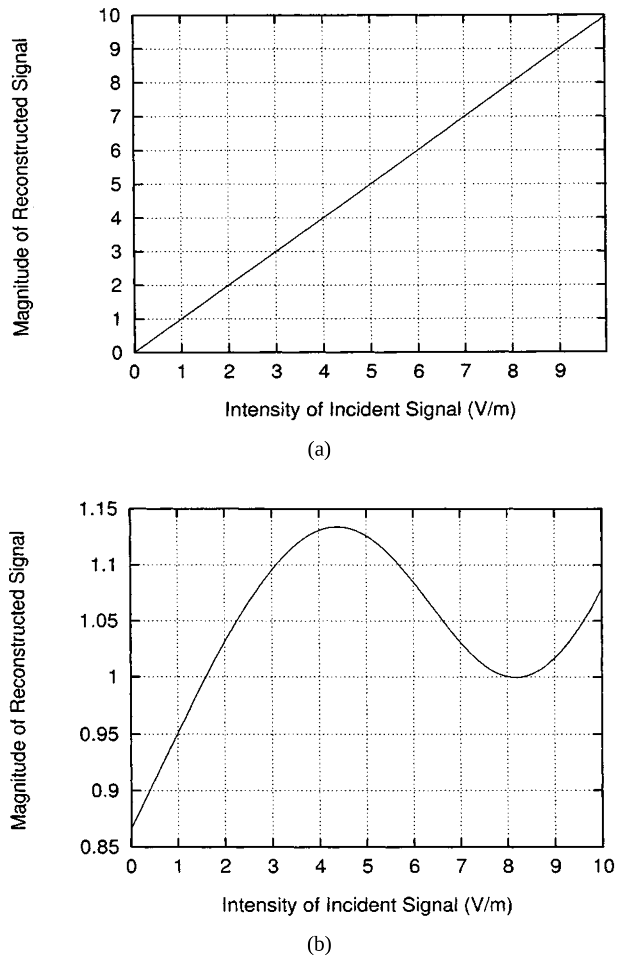

Fig. 4. Signal recovery in the (a) absence and (b) presence of mutual coupling. Example 1.

D. Example 2: Constant Signal

In the second example, the signal is kept constant at 1.0 V/m as given in Table II. The intensity of first jammer arriving from $\phi = 75°$ is varied from 1.0 V/m (0 dB with respect to the signal) to 1000.0 V/m (60 dB) in steps of 5 V/m. The same scenarios of Example 1 are compared. If the jammers are properly nulled, we expect the reconstructed signal to have no residual jammer component. Therefore, as the jammer strength is increased, we expect the reconstructed signal to remain constant.

Fig. 5(a) presents the results of using the receiving algorithm when mutual coupling is absent. The magnitude of the reconstructed signal is indistinguishable from the expected value of 1.0 V/m. This figure demonstrates that in the absence of mutual coupling, the receiving algorithm is highly accurate and can null a strong jammer.

Fig. 5(b) shows the results of using the measured voltages that are affected by mutual coupling. The magnitude of the reconstructed signal varies approximately linearly with respect to the intensity of the jammer. This is because the strong jamming is not nulled and the residual jammer component completely overwhelms the signal.

The reason the signal cannot be recovered when mutual coupling is taken into account can be visually understood by comparing the adapted beam patterns in the ideal case of no mu-

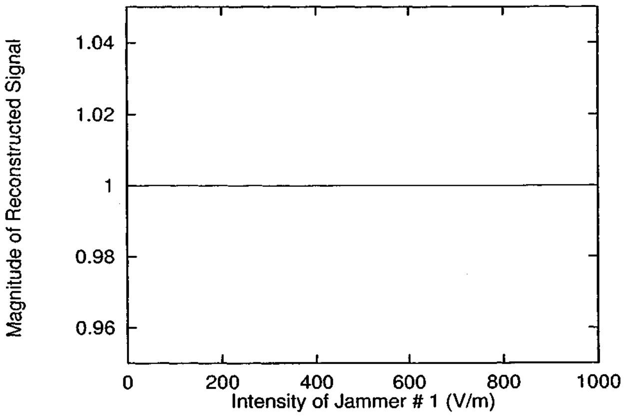

(a)

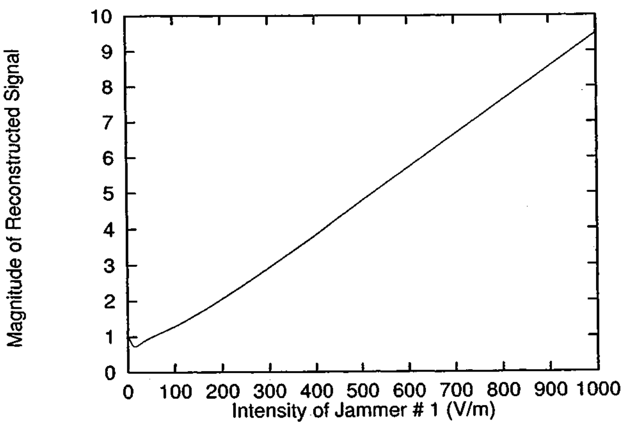

(b)

Fig. 5. Signal recovery in the (a) absence and (b) presence of mutual coupling. Example 2.

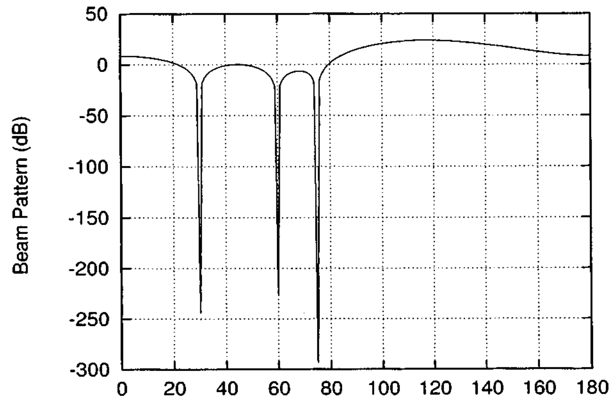

(a)

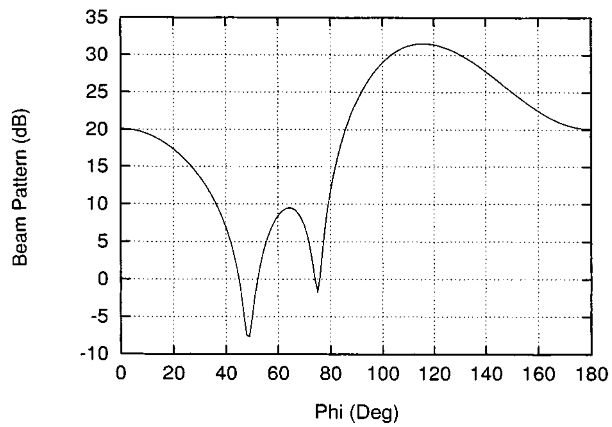

(b)

Fig. 6. Beam patterns in the (a) absence and (b) presence of mutual coupling.

tual coupling with the case where mutual coupling is present. In Fig. 6(a) we see the beam pattern in the ideal case. The pattern clearly displays the three deep nulls at the directions of the interference. The high sidelobes are in the region where there is no interference. Because of the deep nulls, the strong interference can be completely nulled and the signal recovered correctly.

Fig. 6(b) shows the beam pattern when the mutual coupling is taken into account. As is clear, the gain of the antenna in the signal direction is considerably reduced, the pattern nulls are shallow and are displaced from the desired locations. The shallow nulls result in the inadequate nulling of the interference, hence, the signal cannot be recovered.

The two examples presented here illustrate the importance of the problem at hand. When mutual coupling is taken into account not only is the main beam of the adaptive array is pointed in the wrong direction, but also the ability to form deep nulls in the directions of the interference is considerably rediuced.

In summary, the direct data domain algorithm of [2] is a promising alternative to the traditional classical statistical adaptive algorithms. However, using the voltages measured at the ports of the array yields incorrect results and the mutual coupling between the elements undermines the ability of the algorithm to suppress interference.

The next section presents a technique to compensate for the effects of mutual coupling for linear dipole arrays. This technique is demonstrated to be more effective than the compensation technique of [5].

IV. Elimination of Mutual Coupling

Most adaptive algorithms assume that each element in the array is independent of the other elements in the array. The mutual coupling arises due to the reradiation of the incident fields from the elements themselves. To eliminate the effects of mutual coupling, we begin by realizing that the MoM voltages of (4) are related directly to the incident fields and so are not affected by mutual coupling. The approach here will be to recreate some part of the MoM voltage vector from the given measured voltages.

The MoM analysis results in a matrix equation that relates the coefficients of the current expansion to the MoM voltages through the admittance matrix. Since the MoM impedance and admittance matrices are independent of the incident fields, they can be evaluated *a priori*.

The measured voltages at the ports of the antenna are related to the current coefficients by (5). Using this equation and (2), the N_e-dimensional vector of measured voltages can be written as

$$[V]_{\text{meas}} = [\mathbf{Z}_L][\mathbf{Y}_{\text{port}}][V] \qquad (9)$$

where $[\mathbf{Z}_L]$ is the $N_e \times N_e$ diagonal matrix with the load impedances at its entries and $[\mathbf{Y}_{port}]$ is the matrix with the rows of $[\mathbf{Y}]$ that correspond to the ports of the array. $[V]$, the MoM voltage vector is of order N, i.e., the number of unknowns in the MoM analysis. $[\mathbf{Y}_{\rm port}]$ is a rectangular matrix of order $N_e \times N$ with $N > N_e$. Since $[\mathbf{Y}_{\rm port}]$ is a rectangular matrix with more columns than rows, the (9) represents an underdetermined system of equations. Our goal is to estimate some part of $[V]$ given $[V]_{\rm meas}$. Therefore, we need a method to collapse the $N_e \times N$ matrix $[\mathbf{Y}_{\rm port}]$ to a $N_e \times N_e$ matrix.

The proposed method is most easily understood when illustrated with an example. If P unknowns are used per wire element $N = N_e P$. Consider the case with $N_e = 2$ and $P = 3$. Then $N = 6$ and basis function 2 corresponds to the port on the first element while basis function 5 to the port on the second element. In this case, (9) can be written as

$$\begin{bmatrix} V_{\rm meas_1} \\ V_{\rm meas_2} \end{bmatrix} = \begin{bmatrix} Z_L & 0 \\ 0 & Z_L \end{bmatrix} \cdot \begin{bmatrix} Y_{21} & Y_{22} & Y_{23} & Y_{24} & Y_{25} & Y_{26} \\ Y_{51} & Y_{52} & Y_{53} & Y_{54} & Y_{55} & Y_{56} \end{bmatrix} \begin{bmatrix} V_1 \\ V_2 \\ V_3 \\ V_4 \\ V_5 \\ V_6 \end{bmatrix}. \tag{10}$$

If the signal and all the jammers are incident from approximately the same elevation θ, the entries in $[V]$ are not all independent of each other. From (4), if weighting functions i and $(i+1)$ belong to the same array element

$$V_{i+1} = (e^{jk\Delta z \cos\theta}) V_i. \tag{11}$$

Letting $\alpha = e^{jk\Delta z \cos\theta}$, we have

$$V_1 = e^{-jk\Delta z \cos\theta} V_2 = \alpha^{-1} V_2 \tag{12}$$

$$V_3 = e^{jk\Delta z \cos\theta} V_2 = \alpha V_2 \tag{13}$$

$$V_4 = e^{-jk\Delta z \cos\theta} V_5 = \alpha^{-1} V_5 \tag{14}$$

$$V_6 = e^{jk\Delta z \cos\theta} V_5 = \alpha V_5. \tag{15}$$

Therefore, (10) can be reduced to

$$\begin{bmatrix} V_{\rm meas_1} \\ V_{\rm meas_2} \end{bmatrix} = \begin{bmatrix} Z_L & 0 \\ 0 & Z_L \end{bmatrix} \cdot \begin{bmatrix} \alpha^{-1}Y_{21} + Y_{22} + \alpha Y_{23} & \alpha^{-1}Y_{24} + Y_{25} + \alpha Y_{26} \\ \alpha^{-1}Y_{51} + Y_{52} + \alpha Y_{53} & \alpha^{-1}Y_{54} + Y_{55} + \alpha Y_{56} \end{bmatrix} \cdot \begin{bmatrix} V_2 \\ V_5 \end{bmatrix} \tag{16}$$

$$\Rightarrow [V]^{\rm meas} = [\mathbf{B}][V'] \tag{17}$$

where $[V']$ is the vector of length N_e whose entries are the MoM voltages that correspond to the ports and $[\mathbf{B}]$ is the $N_e \times N_e$ matrix that relates the measured voltages to $[V']$. Equation (16) is a relation between the measured voltages and the MoM voltages that correspond to the ports of the array. In a practical application, the measured voltages are the given quantities and are affected by mutual coupling. The MoM voltages on the right-hand side of (16) are the voltages that are directly related to the incident fields and so are free from the effects of mutual coupling. Both vectors are of order N_e, the number of ports. Therefore, this equation can be easily solved for the MoM voltages corresponding to the ports of the antenna. Furthermore, if the elevation angle of interest (θ) is fixed, the matrix $[\mathbf{B}]$ can be evaluated *a priori*. Hence, the computational cost of eliminating the mutual coupling is the limited to the solution of a small matrix equation.

The open circuited voltages are the voltages measured at the ports of the array if the ports were open circuited. In [5], the authors assume that these voltages are free of the effects of mutual coupling. However, the open circuit voltage at a particular element is the voltage measured *in the presence of* the other open circuited elements. Therefore, the effect of mutual coupling has been reduced but not eliminated. Mutual coupling can be assumed to have been eliminated only when there is nothing impeding the path of the incident fields—in effect, not even the array itself.

A. Numerical Examples

In this section, the formulation presented above to eliminate the effects of mutual coupling is tested on four examples. The first two examples are the same as the examples used to demonstrate the effect of mutual coupling in Section III-B. For these two examples, the use of open circuit voltages as suggested by [5] is compared with the use of the voltages found from (17).

B. Example 1: Constant Jammers

The seven-element array defined in Table I receives a signal corrupted by three jammers. The base signal and jammer strengths are as given in Table II. The magnitude of the incident signal is varied from 0 V/m to 10.0 V/m in steps of 0.05 V/m while maintaining jammer intensities constant as given in Table II. For each value of the signal intensity the MoM voltage vector is evaluated to yield the measured voltages. The measured voltages and the signal DOA are treated as the known quantities.

Using the measured voltages and MoM admittance matrix, the open-circuit voltages are obtained [14]. These open circuit voltages are passed to the direct-data domain algorithm described in Section III-A and an attempt is made to recover the signal. It is expected that the recovered signal varies linearly with the intensity of the incident signal. Fig. 7(a) presents the results of using the open-circuit voltages. The expected linear relationship is clearly seen, implying that the jammers have been nulled and the signal recovered correctly. The numerical value of the signal is correct within a calibration constant.

In the second scenario, the measured voltages are used to estimate the vector $[V']$ using (17). These voltages are used to recover the signal. Fig. 7(b) shows the results of using the voltages in $[V']$. Again, the expected linear relationship is clearly visible.

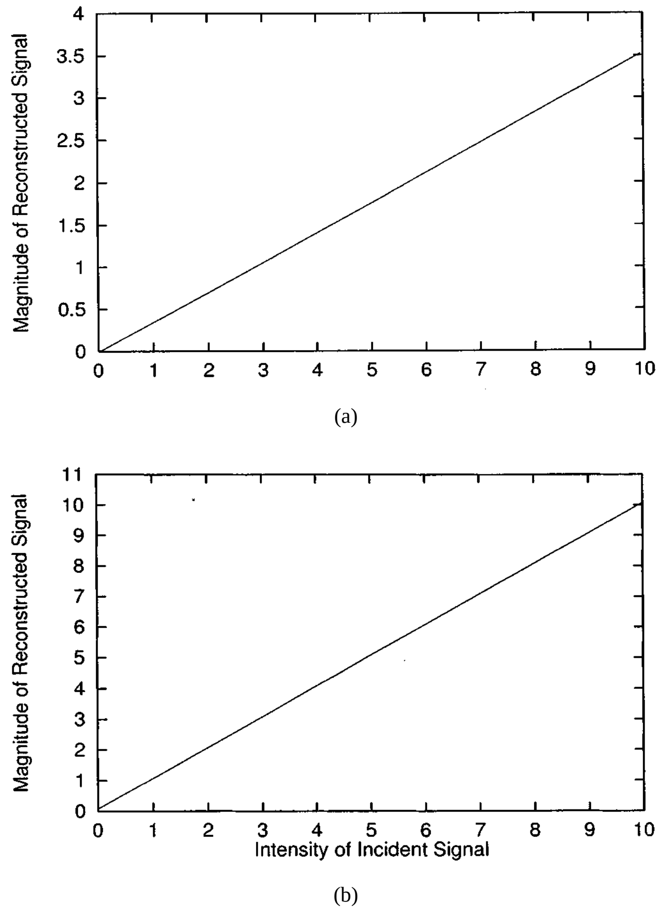

Fig. 7. Signal recovery using (a) open-circuit voltages and (b) after eliminating mutual coupling.

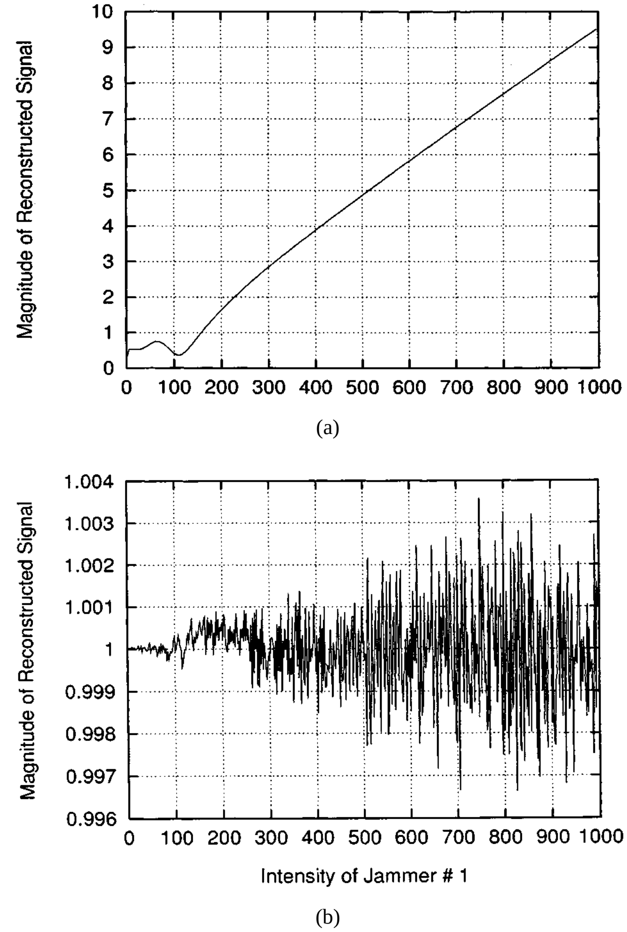

Fig. 8. Signal recovery using (a) open-circuit voltages and (b) after compensating for mutual coupling.

This example has shown that open-circuit voltages do provide some compensation for mutual coupling. The use of open-circuit voltages provides for significantly better signal recovery than using the measured voltages directly, as shown in Fig. 4(b). The technique to eliminate the effects of mutual coupling introduced in Section IV also proves to compensate for mutual coupling.

In this example, however, the interference was relatively weak. A more stringent test for both compensation techniques is to check their ability to suppress strong interference.

C. Example 2: Constant Signal

In the second example, the intensity of the incident signal is held constant at 1.0 V/m. The intensity of the first jammer is varied from 1.0 V/m to 1000 V/m (60 dB above the signal) in steps of 5 V/m. For each value of the jammer intensity, the MoM voltage vector is calculated and the measured voltages are calculated. In the first scenario, the measured voltages are used to find the open-circuit voltages. The open-circuit voltages are passed to the direct-data domain algorithm of [2]. In the second scenario, (17) is used to find the voltage vector $[V']$. These voltages are used to recover the signal and null the jammers using the same algorithm. If the jammers are properly nulled, the reconstructed signal magnitude should remain constant as a function of jammer strength.

Fig. 8(a) presents the results when the open-circuit voltages are used to recover the signal. As can be seen, the recovered signal shows a near linear relationship as a function of jammer strength. This indicates that the jammer has not been adequately nulled and the residual jammer strength has overwhelmed the signal.

The results of compensating for the mutual coupling using the technique presented in this paper is shown in Fig. 8(b). The magnitude of the reconstructed signal varies between 0.996 V/m and 1.004 V/m, i.e., the error in the signal recovery is very small. This figure shows that the strong jammer has been effectively nulled and the signal can be reconstructed.

The reason that using the open-circuit voltages is inadequate to compensating for the mutual coupling while the technique presented here is adequate is illustrated using the adapted beam patterns in the two cases. The adapted beam pattern associated with using the open-circuit voltages is shown in Fig. 9(a). The nulls are placed in the correct locations. However, they are shallow, resulting in the inadequate nulling of the interference.

The beam pattern associated with compensating for the mutual coupling using the technique presented in this paper is shown in Fig. 9(b). The nulls are deep and placed in the correct directions. This demonstrates that the mutual coupling has been suppressed enough so as to null even a strong jammer.

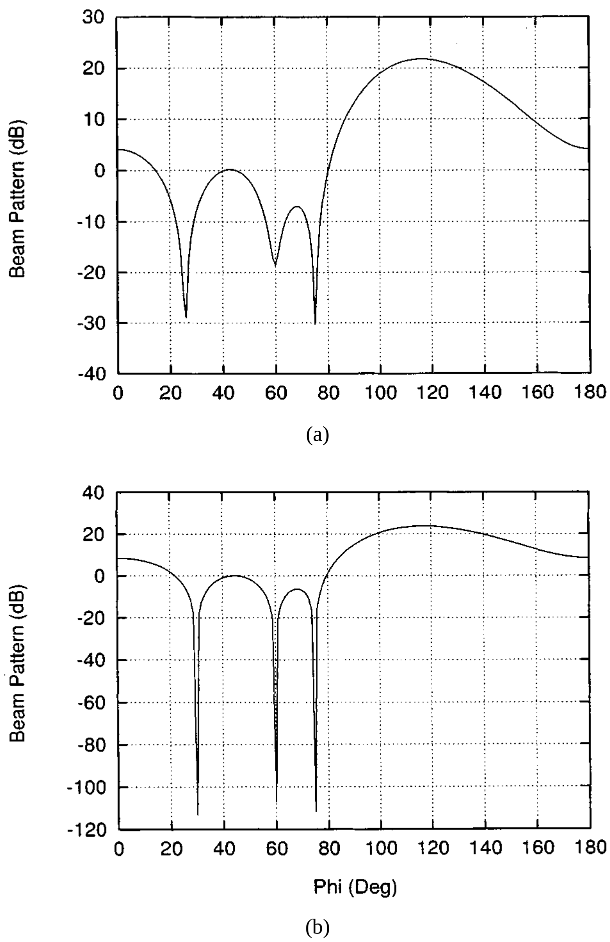

Fig. 9. Beam patterns using (a) the open-circuit voltages and (b) after compensating for mutual coupling.

Figs. 7–9 allow us to conclude that using the open-circuit voltages does reduce the effect of mutual coupling somewhat. However, the reduction is inadequate to suppress strong interference. This is because the open-circuit voltage at an array element is the voltage in the presence of the other open-circuited elements. The technique presented in this paper proves to be far superior in compensating for mutual coupling. This is because by using multiple basis functions per antenna element, the mutual coupling information has been represented accurately.

D. Example 3: Effect of Noise

The examples presented above illustrate the effects of mutual coupling and ignored the additive noise at each antenna element. This example presents the effect of thermal noise on the adaptive algorithm. The noise is additive and is modeled as a Gaussian random variable. The noise at any element is assumed independent of the noise at the other elements. Since the noise introduces a random component to the data, comparisons will be made in terms of averages over many random samples.

In this example, a 13-element array of thin half-wavelength long wire dipoles receives a signal corrupted by three jammers as given in Table III. The z-directed dipoles each have radius $\lambda/200$ and are spaced a half-wavelength apart. Each wire is centrally loaded with a 50 Ω resistance. Seven unknowns per wire are used in the MoM analysis, leading to a total of 91 unknowns.

TABLE III
SIGNAL AND JAMMER VALUES. EXAMPLE 3

	Magnitude (V/m)	Phase	DOA
Signal	1.0	0.0	85^o
Jammer # 1	2000.0	0.0	135^o
Jammer # 2	1.5	0.0	60^o
Jammer # 3	2.0	0.0	100^o

The signal-to-noise ratio was set at 13 dB. Note that jammer 1 is a strong jammer (66 dB with respect to the signal).

For each of the 13 channels, a complex Gaussian random variable is added to the measured voltages due to the signal and jammers. This set of voltages, affected by noise, is passed to the signal recovery routine described in Section IV. This procedure is repeated 500 times with different noise samples. These 500 samples are used to find the average and variance. The output signal to interference plus noise ratio (SINR) in decibels is defined as

$$SINR_{\text{out}} = 10.0 \log \left[\frac{|S|^2}{|\text{bias}|^2 + \text{var}} \right]. \tag{18}$$

The results of the above simulation are presented in Table IV.

When the measured voltages are used directly to recover the signal mainly due to the high bias in the estimate of the signal, the output SINR is only 6.355 dB. The high bias can be directly attributed to the inadequate nulling of the strong jammer. However, when the mutual coupling is eliminated using the technique presented in this paper, the jammers are completely nulled yielding accurate estimates of the signal. The total interference power is suppressed to nearly 20 dB below the signal.

The examples presented here demonstrate that the method proposed in this section is an effective compensation technique to deal with the effects of mutual coupling. Using the MoM with multiple basis functions per element allows us to reduce the mutual coupling to an extent where it is inconsequential.

V. CONCLUSIONS

This paper has demonstrated that, for the development of practical direct-data domain algorithms, the electromagnetic nature of the array must be taken into account. We have shown that the mutual coupling between the elements of the array causes adaptive algorithms to fail. This problem is associated with both covariance matrix approaches (stated earlier by [5]) and direct-data domain approaches (investigated here).

To properly characterize the antenna the MoM is used. Previously published work in this area has used only one basis function per element. However, this is usually inadequate for an accurate antenna analysis. The use of multiple basis functions per element in a practical manner is a major advance over previously published methods.

The mutual coupling is eliminated by recognizing that the MoM voltage vector is free from mutual coupling. By using a relationship between the entries of the MoM voltage vector, a square matrix equation is developed between the given measured voltages and the relevant entries of the MoM voltage vector. It is shown that this method works very well in the

TABLE IV
RESULTS OF 500 SIMULATIONS. EXAMPLE 3

	Without compensating for mutual coupling	After compensating for mutual coupling
Input Signal to Noise Ratio	$13dB$	$13dB$
Number of samples	500	500
True Value	(1.0,0.0) V/m	(1.0,0.0) V/m
Mean of 1000 estimates	(0.93337,0.49295) V/m	(1.00379,-0.00298) V/m
Bias of estimate	(-0.06663,0.49295) V/m	(0.00379,-0.00298)
Variance of estimates	0.010448	0.0103797
Output SINR	6.35526 dB	19.86559

presence of strong interfering sources. Furthermore, it is shown that the proposed technique is superior to the earlier suggested method of using the open circuit voltages.

In summary, this paper has investigated a topic that is very important to the development of practical adaptive algorithms. The proposed method is easy to implement and does not add an inordinate computational burden on the adaptive process.

REFERENCES

[1] R. A. Monzingo and T. W. Miller, *Introduction to Adaptive Arrays*, New York: Wiley, 1980.

[2] T. K. Sarkar and N. Sangruji, "An adaptive nulling system for a narrow-band signal with a look-direction constraint utilizing the conjugate gradient method," *IEEE Trans. Antennas Propagat.*, vol. 37, pp. 940–944, July 1989.

[3] S. Park and T. K. Sarkar, "A deterministic eigenvalue approach to space time adaptive processing," *Digital Signal Processing, Rev. J.*, vol. 6, no. 3, pp. 185–194, 1996.

[4] R. Schneible, "A least squares approach to radar array adaptive nulling," Ph.D. dissertation, Syracuse University, Syracuse, NY, 1996.

[5] I. J. Gupta and A. A. Ksienski, "Effect of mutual coupling on the performance of adaptive arrays," *IEEE Trans. Antennas Propagat.*, vol. AP-31, pp. 785–791, Sept. 1983.

[6] S. A. Schelkunoff and H. T. Friis, *Antenna Theory and Practice*, New York: Wiley, 1966.

[7] R. S. Adve, "Elimination of the Effects of Mutual Coupling in Adaptive Thin Wire Antennas," Ph.D. dissertation, Syracuse Univ., Syracuse, NY, Dec. 1996.

[8] M. L. Leou, C. C. Yeh, and D. R. Ucci, "Bearing estimations with mutual coupling present," *IEEE Trans. Antennas Propagat.*, vol. 37, pp. 1332–1335, Oct. 1989.

[9] B. Himed, "Application of the Matrix Pencil approach to direction finding," Ph.D. dissertation, Syracuse University, Syracuse, NY, May 1990.

[10] B. Friedlander and A. J. Weiss, "Direction finding in the presence of mutual coupling," *IEEE Trans. Antennas Propagat.*, vol. 39, pp. 273–284, Mar. 1991.

[11] K. M. Pasala and E. M. Friel, "Mutual coupling effects and their reduction in wideband direction of arrival estimation," *IEEE Trans. Aerosp. Electron. Syst.*, vol. 30, pp. 1116–1122, Apr. 1994.

[12] E. M. Friel, "Direction finding with compensation for electromagnetic effects," Ph.D. dissertation, University of Dayton, Dayton, OH, Dec. 1995.

[13] B. J. Strait, T. K. Sarkar, and D. C. Kuo, "Special programs for analysis of radiation by wire antennas," Syracuse Univ., Tech. Rep. AFCRL-TR-73-0399, June 1973.

[14] A. R. Djordjevic *et al.*, *Analysis of Wire Antennas and Scatterers: Software and User's Manual*. Norwood, MA: Artech House, 1995.

Raviraj S. Adve (S'88–M'97) was born in Bombay, India. He received the B.Tech. degree in electrical engineering from Indian Institute of Technology (IIT), Bombay, in 1990, and the Ph.D. degree from Syracuse University, Syracuse, NY, in 1996.

He is currently working for Research Associates for Defense Conversion (RADC) Inc., Maroy, NY, under contract with the Air Force Research Laboratory, Rome, NY. His research interests include practical adaptive signal processing algorithms for airborne radar and wireless applications and the applications of numerical electromagnetics to adaptive signal processing. He has also investigated the applications of signal processing techniques to numerical and experimental electromagnetics.

Tapan Kumar Sarkar (S'69–M'76–SM'81–F'92) received the B.Tech. degree from the Indian Institute of Technology, Kharagpur, India, in 1969, the M.Sc.E. degree from the University of New Brunswick, Fredericton, Canada, in 1971, and the M.S. and Ph.D. degrees from Syracuse University, Syracuse, NY, in 1975.

From 1975 to 1976 he was with the TACO Division of the General Instruments Corporation, Sherburne. He was with the Rochester Institute of Technology, Rochester, NY, from 1976 to 1985. He was a Research Fellow at the Gordon McKay Laboratory, Harvard University, Cambridge, MA, from 1977 to 1978. He is now a Professor in the Department of Electrical and Computer Engineering, Syracuse University. His current research interests deal with numerical solutions of operator equations arising in electromagnetics and signal processing with application to system design. He is a registered Professional Engineer in the State of New York. He is on the editorial board of *Journal of Electromagnetic Waves and Applications*. He has authored or coauthored more than 210 journal articles and numerous conference papers and has written chapters in ten books including, *Iterative and Self Adaptive Finite-Elements in Electromagnetic Modeling* (Norwood, MA: Artech House, 1998).

Dr. Sarkar received the Best Paper Award of the IEEE TRANSACTIONS ON ELECTROMAGNETIC COMPATIBILITY in 1979 and at the 1997 National Radar Conference. He was an Associate Editor for feature articles of the *IEEE Antennas and Propagation Society Newsletter* and he was the Technical Program Chairman for the 1988 IEEE Antennas and Propagation Society International Symposium and URSI Radio Science Meeting. He has been appointed U.S. Research Council Representative to many URSI General Assemblies. He was the Chairman of the Intercommission Working Group of International URSI on Time Domain Metrology (1990–1996). He is a member of Sigma Xi and International Union of Radio Science Commissions A and B. He received the title Docteur Honoris Causa from Universite Blaise Pascal, Clermont Ferrand, France in 1998. He obtained one of the "Best Solution" awards in May 1977 at the Rome Air Development Center (RADC) Spectral Estimation Workshop.